ACS Chemical Neuroscience

Research Article

pubs.acs.org/chemneuro

Enhanced Dopamine Release by Dopamine Transport Inhibitors Described by a Restricted Diffusion Model and Fast-Scan Cyclic Voltammetry

Alexander F. Hoffman,* Charles E. Spivak, and Carl R. Lupica

Electrophysiology Research Section, Cellular Neurobiology Branch, National Institute on Drug Abuse Intramural Research Program, Baltimore, Maryland 21224, United States

Supporting Information

ABSTRACT: Fast-scan cyclic voltammetry (FSCV) using carbon fiber electrodes is widely used to rapidly monitor changes in dopamine (DA) levels *in vitro* and *in vivo*. Current analytical approaches utilize parameters such as peak oxidation current amplitude and decay times to estimate release and uptake processes, respectively. However, peak amplitude changes are often observed with uptake inhibitors, thereby confounding the interpretation of these parameters. To overcome this limitation, we demonstrate that a simple five-parameter, two-compartment model mathematically describes DA signals as a balance of release (r/k_e) and uptake (k_u), summed with adsorption (k_{ads} and k_{des}) of DA to the carbon electrode surface. Using nonlinear regression, we demonstrate that our model precisely describes measured DA signals obtained in brain slice recordings. The parameters extracted from these curves were then validated using pharmacological manipulations that selectively alter vesicular release or DA transporter (DAT)-mediated uptake. Manipulation of DA release through altering the Ca^{2+}/Mg^{2+} ratio or adding tetrodotoxin reduced the release parameter with no effect on the uptake parameter. DAT inhibitors methylenedioxypyrovalerone, cocaine, and nomifensine significantly reduced uptake and increased vesicular DA release. In contrast, a low concentration of amphetamine reduced uptake but had no effect on DA release. Finally, the kappa opioid receptor agonist U50,488 significantly reduced vesicular DA release but had no effect on uptake. Together, these data demonstrate a novel analytical approach to distinguish the effects of manipulations on DA release or uptake that can be used to interpret FSCV data.

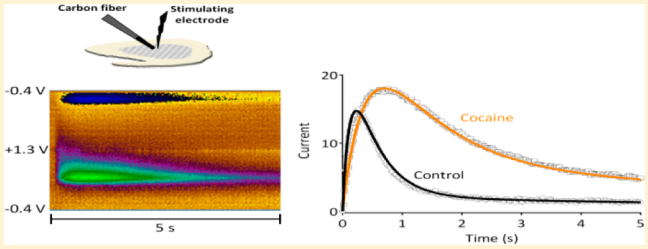

KEYWORDS: *Voltammetry, kinetics, dopamine transporter, drug abuse, cathinones, brain slice*

Fast-scan cyclic voltammetry (FSCV) using carbon fiber electrodes has long been used to monitor dopamine (DA) levels both *in vitro* and *in vivo*. Since sampling intervals of <10 ms are feasible using this technique,[1,2] the dynamics of both DA release and uptake can be quantified. Mathematical solutions incorporating Michaelis−Menten kinetics have been used to quantify DA signals,[3−6] although this requires untested assumptions regarding the mechanisms of a drug's actions and specialized curve fitting algorithms. A simpler description of currents arising from DA oxidation involves measuring parameters such as peak amplitude and decay time.[7] The peak amplitude of the oxidation current measured at the carbon fiber electrode has historically been used as an index of the amount of DA released, whereas the decay of this signal is used to assess DA transporter (DAT)-mediated uptake. However, a confounding of these variables is likely because DAT inhibitors, which should alter only DA uptake, also typically *increase* the peak signal amplitude.[4,8,9] Moreover, the typical estimation of uptake is performed using a single-exponential decay time constant (tau, τ), but this is often confounded by the fact that DA currents do not fully decay back to prestimulus baselines, an artifact that likely reflects trapping of DA at the electrode surface due to adsorption.[10−12] For these reasons, a simple model that unequivocally resolves release and uptake components of FSCV signals would aid in measuring the effects of behavioral and pharmacological manipulations on DA dynamics. In the present study, we have adapted and simplified the "restricted diffusion"-based model recently proposed by Walters et al.[11,12] and demonstrate its application to the measurement of DA release and uptake in brain slices, where experimental conditions permit resolution of release and uptake components. Our model can be implemented with a variety of software packages that perform nonlinear curve fitting analysis, making it accessible to a number of laboratories that perform FSCV.

RESULTS AND DISCUSSION

The rapid sampling frequency of FSCV recording should, in principle, allow for resolution of DA release and uptake. Most prior studies have relied on measuring the peak amplitude of the DA signal as an indicator of release and utilized the time course of the falling phase of the DA signal as a quantitative measure of

Received: October 20, 2015
Accepted: March 19, 2016
Published: March 28, 2016

DOI: 10.1021/acschemneuro.5b00277
ACS Chem. Neurosci. 2016, 7, 700−709

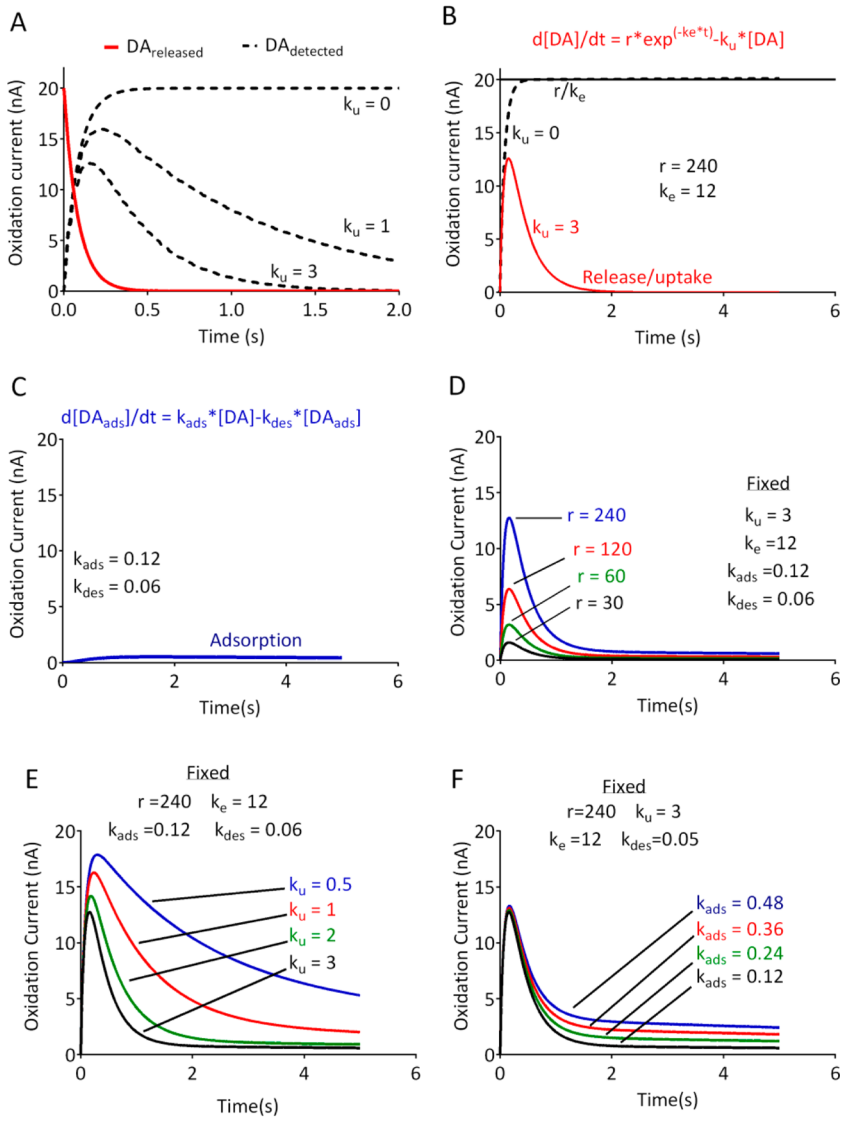

Figure 1. DA release and uptake modeled with five parameters. (A) Kinetic scheme underlying the model. Red line indicates the DA released into the tissue, and dashed lines indicate the DA detected at the carbon fiber electrode. As described in the text, the transfer of DA from the inner compartment is mirrored by its appearance in the outer compartment. In the absence of any uptake ($k_u = 0$), the asymptotic portion of the curve for DA detection will reflect the initial DA released at time 0. Increasing uptake will reduce the peak amplitude of the signal and force the signal away from the asymptote. (B) Mathematical representation of the kinetic model (see Methods). Solid line shows the release term r/k_e, which represents the maximal release in the absence of any uptake (e.g., $k_u = 0$, dashed line). Note the difference between r/k_e and the peak amplitude of the signal when uptake is present (red trace). (C) Equation that models DA adsorption to the electrode. (D–F) Simulated DA current vs time profile, which reflects the sum of the curves using the parameters and equations from (B) and (C). Curves were modeled by using fixed parameters as indicated and varying r, k_u, or k_{ads}, respectively. Note the distinct changes in the shapes of the curves produced by the changes in each parameter. Parameters were chosen based on typical values obtained in brain slices.

uptake. These assumptions present problems, however, since uptake clearly influences the peak height of the signal (present study and refs 4 and 13). This likely reflects the fact that uptake is ongoing and occurs more rapidly than DA is detected at the electrode using FSCV (50–100 ms). For this reason, it is preferable to have a parameter that cleanly distinguishes release from uptake processes. Here, we describe a model of FSCV signals that unambiguously distinguishes vesicular DA release from uptake. Adapting a restricted diffusion model developed by Walters et al.,[11,12] we demonstrate that a simple five-parameter scheme (r, k_e, k_u, k_{ads}, and k_{des}) is sufficient to adequately describe current vs time waveforms obtained in striatal brain slices. Using pharmacological approaches in brain slices, we validate the quantitative application of this model using both known release modulators (Ca^{2+}, TTX) and uptake inhibitors (methylenedioxypyrovalerone [MDPV], cocaine, nomifensine, and amphetamine). In addition, we utilize this model to demonstrate that kappa opioid receptor (KOR) activation inhibits DA release but does not affect DA uptake, consistent with previous FSCV studies.[14,15]

Model. Our objective was to develop a model that describes the DA oxidation current vs time profile in a way that (1) distinguishes release from uptake processes, (2) accounts for the failure of the signals to decay back to prestimulus baseline ("tails"), and (3) utilizes the fewest number of parameters so that each can be unambiguously determined by minimizing least-squares fits to the data sets. As shown in Figure 1, a simplified five-parameter model was chosen based on simultaneous

DOI: 10.1021/acschemneuro.5b00277
ACS Chem. Neurosci. 2016, 7, 700–709

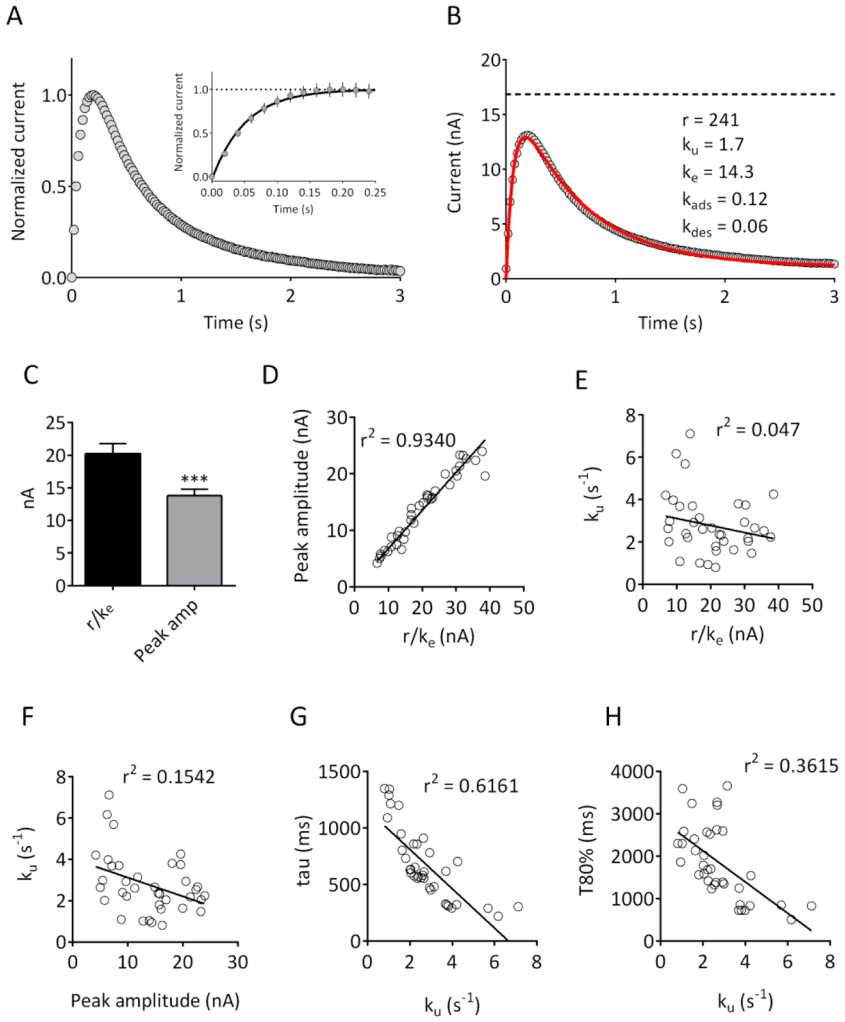

Figure 2. Fitting of the model to DA signals obtained in rat brain slices. (A) Averaged current responses obtained in 37 brain slices obtained from 10 rats. Peak current was normalized for each slice. In this and subsequent figures, data are aligned so that time 0 corresponds to delivery of a single 1 ms duration constant current pulse. The inset plot shows the initial rising phase of the current on an expanded time scale. Note that the increase in current was seen in the first data point sampled following stimulation (20 ms) and reached a plateau within 150−200 ms. (B) Raw data, from the same slices, fitted (solid red line) using the model described in the text. The parameters obtained are indicated; the dashed line represents r/k_e. (C) Comparison of r/k_e with peak amplitude values obtained in the same slices demonstrates that peak amplitude values are significantly lower than r/k_e (n = 37; $p < 0.001$, two-tailed paired t-test). (D, E) r/k_e is strongly correlated with peak amplitude ($p < 0.0001$) but is not correlated with the uptake parameter k_u ($p = 0.1983$). (F) Peak amplitude is significantly correlated with k_u ($p = 0.02$). (G, H) Correlation of the uptake parameter k_u with the decay time constant (tau; $p < 0.0001$), and 80% decay time (T80%; $p < 0.0001$) of the obtained signals.

equations incorporating DA release and uptake and adsorption of DA to the electrode (see Methods). The parameters, which are described further below, are r, k_e, k_u, k_{ads}, and k_{des}. In order to describe the balance between DA release and uptake, we have adopted and modified the restricted diffusion model described by Walters.[11,12] This model, based on previous work by Nicholson and colleagues,[16,17] employs two kinetic compartments: an "inner compartment" into which DA is initially released, followed by an "outer compartment" in which DA is detected by the carbon fiber electrode. In this kinetic scheme, Walters et al. utilize the term k_r to modify ongoing DA release into the inner compartment and the term k_T to account for the transfer of DA to the outer compartment.[11] However, in the case of single-pulse release, the k_r term does not apply and can be eliminated. Therefore, the kinetic terms used by these investigators (k_r and k_T of Walters et al.[11,12]) were eliminated from the model and replaced with an equivalent kinetic model (see Supporting Information). The remaining, simplified kinetic scheme can be summarized as follows

$$[\mathrm{DA}]_{\mathrm{released}} \xrightarrow{k_e} [\mathrm{DA}]_{\mathrm{detected}} \xrightarrow{k_u} [\mathrm{uptake}] \qquad \text{(Scheme 1)}$$

where k_e represents the rate constant for transfer of the DA from the inner compartment to the carbon fiber electrode (replacing both the k_r and the k_T parameters of Walters et al.[11,12]) and k_u represents a first-order uptake rate constant. We choose the term k_e in order to make it clear that this governs the overall rate of transfer of DA to the electrode and thus includes DA diffusion to the carbon fiber. The contribution of diffusion is indicated by the delay in the time following stimulation for the signal to reach its peak amplitude, a process referred to as "overshoot" by Walters et al.[12] Indeed, as shown in Figure 2, although DA is initially detected within the first time point sampled following a single 1 ms electrical pulse, the peak signal detected at the electrode occurs after ∼150−200 ms. This kinetic model can be formally

DOI: 10.1021/acschemneuro.5b00277
ACS Chem. Neurosci. 2016, 7, 700−709

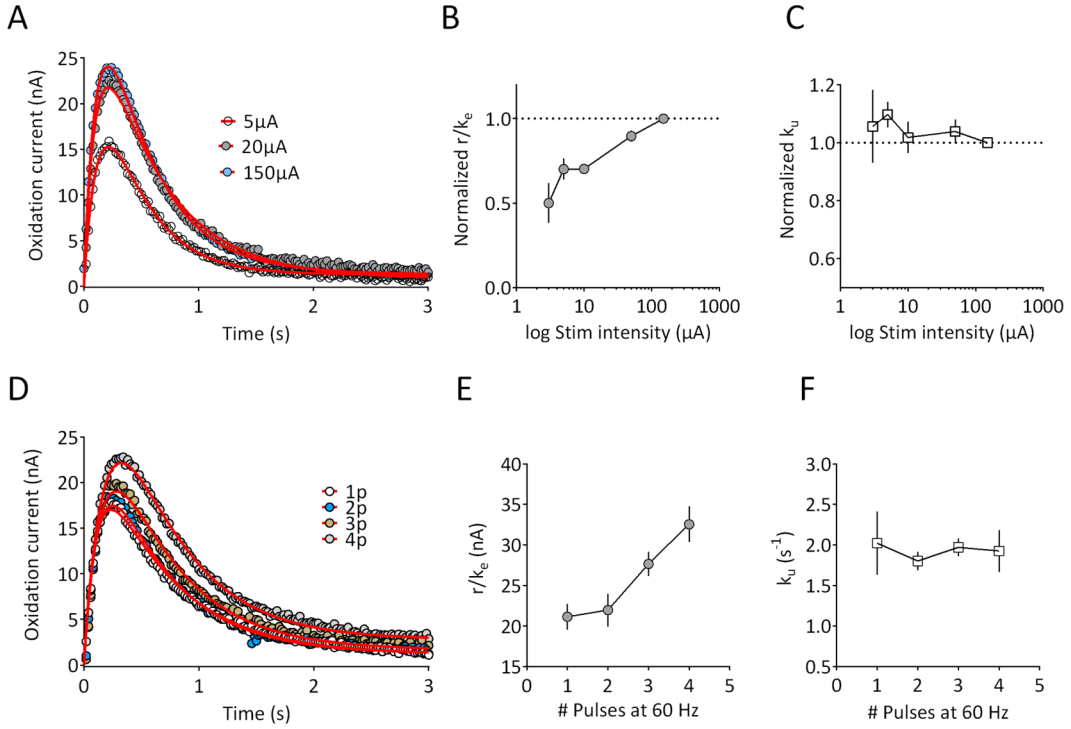

Figure 3. Effect of varying stimulation intensity and number of stimulus pulses on release and uptake parameters. (A) Recording from a striatal slice using single-pulse stimulation (1 ms) delivered at 5, 20, and 150 μA. Data represent the mean of three signals obtained under each condition and are plotted with circles. The fitted curves from which parameters were extracted are shown with the solid red line. (B) Normalized release parameter (r/k_e) as a function of stimulus intensity for all slices (n = 12 from three rats). Data are normalized to the response obtained at 150 μA. A repeated-measures, one-way ANOVA revealed a significant effect of stimulus intensity ($F_{(11,4)} = 21.17$, $p < 0.001$). (C) Normalized uptake parameter (k_u) obtained in the same set of slices. No significant effect of stimulus intensity was observed ($F_{(11,4)} = 0.735$, $p = 0.574$). (D) Recording from a striatal slice using either a single 150 μA pulse or two, three, or four pulses delivered at 60 Hz. Data represent the mean of three signals obtained under each condition and are plotted with circles. The fitted curves from which parameters were extracted are shown with the solid red line. (E) Mean release parameter (r/k_e) plotted as a function of the number of pulses (n = 4 slices from two rats). A repeated-measures, one-way ANOVA revealed a significant effect of pulse number ($F_{(3,3)} = 15.33$, $p < 0.001$) on the release parameter. (F) Mean uptake parameter in the same group of slices. No significant effect of pulse number on the uptake parameter was observed ($F_{(3,3)} = 0.381$, $p = 0.770$). Parameter values for the fitted curves are provided in the Supporting Information.

described by the following system of coupled differential equations:

$$\frac{d[DA]_{released}}{dt} = -k_e \times [DA]_{released}$$

$$\frac{d[DA]_{detected}}{dt} = k_e \times [DA]_{released} - k_u \times [DA]_{detected}$$

A plot of these two equations (Figure 1A) demonstrates that in the absence of any uptake mechanism (e.g., $k_u = 0$) the DA detected at the electrode will eventually reach an asymptotic level that will equal $[DA]_{release}$ at time 0. In terms of the Walters model, following its release, DA is transferred from the inner compartment to the outer compartment, and this reaction proceeds until its completion. As explained by Walters et al.,[11,12] it is assumed that the scheme proceeds in the forward direction (e.g., that DA does not transport back to the site of release). In this kinetic scheme, the addition of an uptake term (k_u) will cause the removal of DA from the $[DA]_{detected}$ compartment, thereby preventing the detected DA from reaching the asymptotic level. As shown in Figure 1, the degree of uptake will clearly influence the observed peak amplitude of the signal. Notably, as the uptake term is increased, the signal will "bend away" sharply from the asymptotic curve, and the amplitude (peak height) of the signal will vary depending on the uptake parameter. In essence, this means that the peak amplitude of the signal will always *underestimate* the maximum (released) DA. A mathematical formulation of the restricted diffusion model was then derived (see Methods, eq 1) and is shown in Figure 1B. Inspection of the current vs time plot clearly demonstrates that the DA detected at the electrode will rise to a maximum value of r/k_e in the absence of any uptake (dashed line in Figure 1B). Regardless of the underlying values of r and k_e, this projected maximum is mathematically equivalent to the initial DA present in the inner compartment. Since the DA in the inner compartment arises directly from DA released from axon terminals,[11,12] solving for this initial DA condition will also solve for the initial DA release, according to the model described above (also see Methods). In the present study, this term is always expressed in nA, but it can be readily converted to μM concentration based on post-electrode calibrations. The clearance of DA by diffusion and transporter-mediated uptake are approximated as first-order processes whose rate constants are summed in the parameter k_u (in units of s^{-1}). Although a Michaelis–Menten term for DAT-mediated uptake[3,5] would, in principle, allow for resolution of uptake and diffusion, we found that the addition of even one more parameter increases the interdependency among the parameters to such an extent that their values can no longer be uniquely determined. In addition, elimination of Michaelis–Menten parameters (K_m and V_{max}) allows for fitting of the raw current vs time data, minimizing the need for calibration factors that may vary with recording conditions.[18,19] The Walters model

DOI: 10.1021/acschemneuro.5b00277
ACS Chem. Neurosci. 2016, 7, 700–709

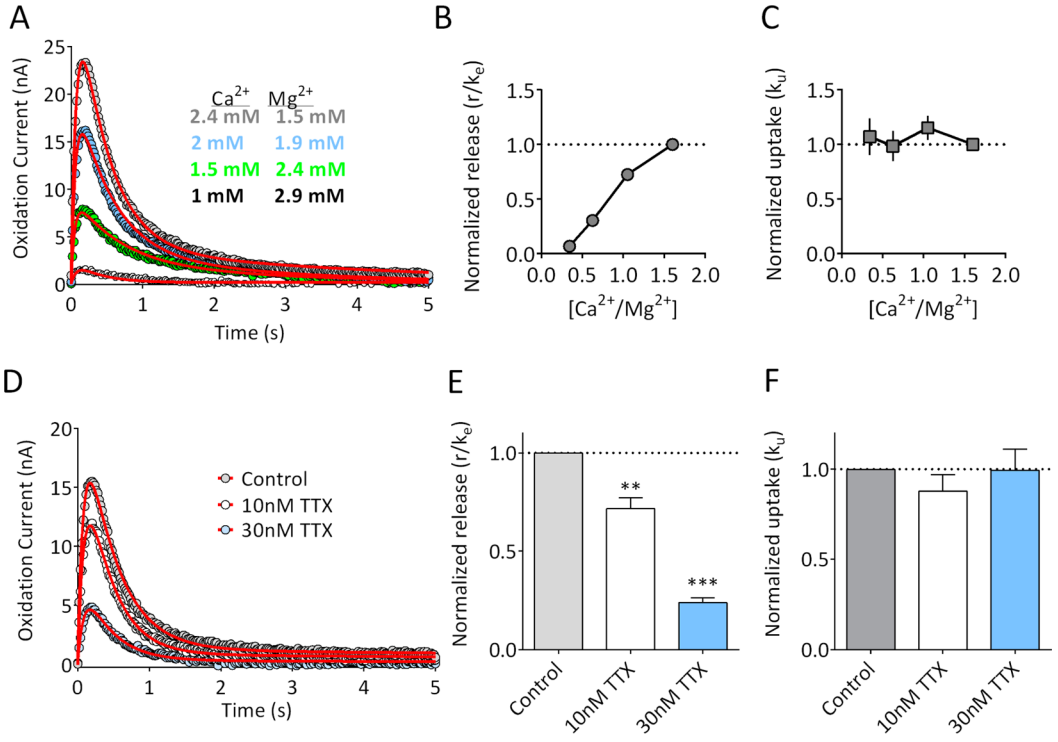

Figure 4. Effect of Ca^{2+}/Mg^{2+} and tetrodotoxin (TTX) on DA release and uptake parameters. (A) Representative recording from a striatal brain slice demonstrating the reduction in the response produced by lowering extracellular Ca^{2+} while raising Mg^{2+} to maintain divalent cation concentrations. Data represent the mean of three signals obtained under each condition and are plotted with circles. The fitted curves from which parameters were extracted are shown with red lines. (B) Release parameter (r/k_e) as a function of the Ca^{2+}/Mg^{2+} ratio ($n = 5$ slices from two rats). Release was significantly reduced by lowering Ca^{2+} and raising Mg^{2+} (RM-ANOVA, $F_{(3,12)} = 83.24$, $p < 0.001$). (C) Uptake parameter k_u was not significantly affected by altering the Ca^{2+}/Mg^{2+} ratio (RM-ANOVA, $F_{(3,12)} = 1.903$, $p = 0.1830$). (D) Representative recording from a striatal brain slice demonstrating the reduction in the response produced by 10 and 30 nM TTX. Data represent the mean of three signals obtained under each condition and are plotted with circles. The fitted curves are shown with the red lines. (E) Summary of the effects of TTX on the release parameter (r/k_e; $n = 5$ slices from two rats). Release was significantly reduced by TTX in a concentration-dependent manner (RM-ANOVA, $F_{(2,8)} = 176$, $p < 0.001$; $^{**}p < 0.01$, $^{**}p < 0.001$ vs control, Dunnett's posthoc). (F) Uptake parameter k_u was not significantly affected by TTX application (RM-ANOVA, $F_{(2,8)} = 0.6935$, $p = 0.5276$). Parameter values for the fitted curves are provided in the Supporting Information.

also accounts for the tails in the current−time curves that are due to DA adsorption (termed "hang-up" by these investigators[11]) using a separate analysis of the tail portion of the curves. Since we also observed these tails, we developed a mathematical solution to account for DA adsorption (Figure 1C) and incorporated this into a model in which all of the parameters (r, k_e, k_u, k_{ads}, and k_{des}) are evaluated by a single-pass least-squares fit. Simulations using this model, using parameters similar to those found under control conditions in brain slices, indicated that changes in release or uptake should be reflected in the shape of the curves (Figure 1D−F), making them suitable for fitting to data sets obtained *in vitro*. It is important to note that changes in the uptake parameter, k_u, clearly affect the peak height of the simulated responses (Figure 1E), confirming that peak amplitudes alone do not adequately describe release.

Comparison of Modeled Parameters with Conventional Parameters. In order to compare our modeled parameters with typical measures obtained using FSCV, we obtained a large number of signals from slices containing the dorsal striatum under control conditions ($n = 37$ slices from 10 rats). A different recording electrode was used in each subject; within each slice, three responses to a 150 μA, 1 ms single-pulse stimulation were averaged. The mean signal from all recordings is shown in Figure 2B, along with the best fit parameters. For each response, we compared the parameters obtained from the model with other parameters commonly used to measure release and uptake. As shown in Figure 2C, the r/k_e value was significantly greater than the measured peak amplitude value ($t = 10.56$, df = 36, $p < 0.001$, paired t-test), consistent with the hypothesis that the amplitude underestimates the initial DA released at time 0. There was a strong correlation between r/k_e and peak amplitude (Pearson's $r^2 = 0.934$, $p < 0.0001$; Figure 2D), as would be expected if both parameters are closely related to the release process. In contrast, r/k_e and k_u were not significantly correlated ($r^2 = 0.047$, $p = 0.1983$; Figure 2E), whereas peak amplitude and k_u demonstrated a small but significant correlation ($r^2 = 0.1542$, $p = 0.02$; Figure 2F). In addition, k_u was significantly correlated with both the decay time constant (tau; $r^2 = 0.6161$, $p < 0.0001$; Figure 2G) and 80% decay time (T80%; $r^2 = 0.3615$, $p < 0.0001$; Figure 2H) parameters commonly used to evaluate uptake.[7] These data suggest that r/k_e and k_u are independent measures of the release and uptake processes, respectively, whereas peak amplitude reflects a combination of both release and uptake.

Validation of the Release Parameter, r/k_e. If r/k_e uniquely reflects DA release, then this parameter should be sensitive to manipulations that selectively affect neurotransmitter release. Therefore, we used physiological and pharmacological manipulations to selectively modify DA release. First, we examined the relationship between stimulus intensity and r/k_e by constructing input−output curves (Figure 3A). Consistent with a higher stimulation intensity recruiting more available terminals for release, the r/k_e parameter showed a significant,

DOI: 10.1021/acschemneuro.5b00277
ACS Chem. Neurosci. 2016, 7, 700−709

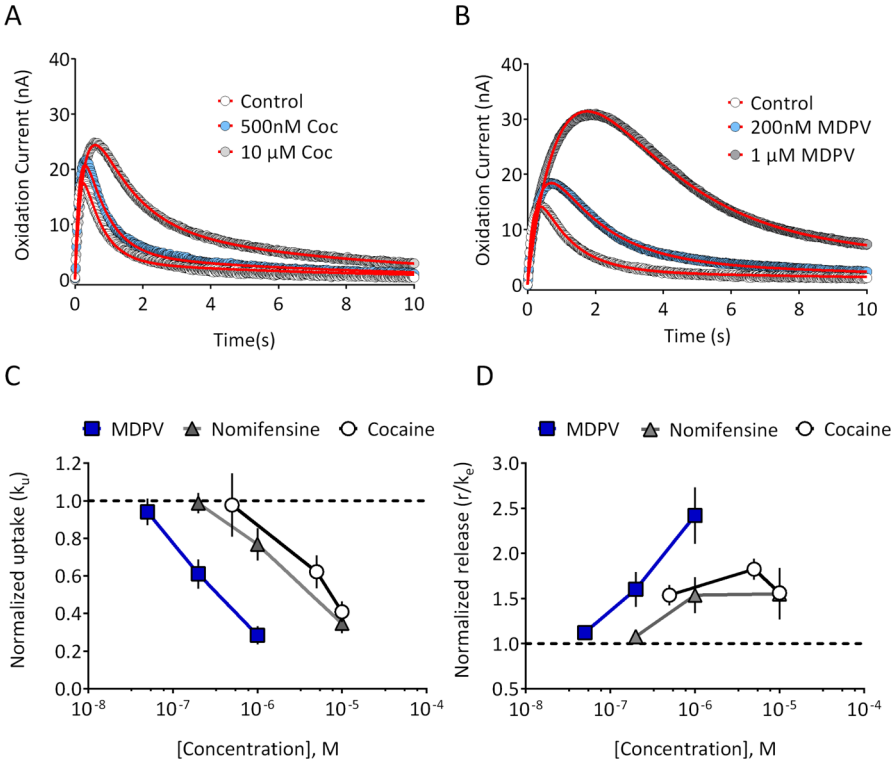

Figure 5. Inhibition of uptake and enhancement of vesicular DA release by DAT inhibitors. (A) Representative recording from a striatal brain slice demonstrating the effects of 500 nM and 10 μM cocaine. Data represent the mean of three signals obtained under each condition and are plotted with circles. The fitted curves are shown with the red line. (B) Effects of MDPV (200 nM and 1 μM) on signals obtained in a different striatal slice. (C) Normalized uptake parameter k_u was reduced in a concentration-dependent manner by MDPV ($n = 7$ slices from 2 rats), cocaine ($n = 8$ slices from three rats), and nomifensine ($n = 7$ slices from two rats). (D) The release parameter was increased in a concentration-dependent manner by MDPV, cocaine, and nomifensine. Parameter values for the fitted curves are provided in the Supporting Information.

stimulus-intensity-dependent increase across all slices tested ($n = 12$, Figure 3B; one-way RM-ANOVA, $F_{(11,4)} = 21.17$, $p < 0.001$). In contrast, the uptake parameter k_u did not significantly differ across the stimulus intensity range (Figure 3C; one way RM-ANOVA, $F_{(11,4)} = 0.735$, $p = 0.574$). As a second physiological approach, we varied the number of stimulus pulses delivered at 60 Hz and compared this to release elicited by a single pulse. As shown in Figure 3D, increasing the number of pulses resulted in an enhanced DA signal. Across all slices tested, there was a significant effect of the number of stimulus pulses on r/k_e ($n = 4$; Figure 3E; one way RM-ANOVA, $F_{(3,3)} = 15.33$, $p < 0.001$), with no effect on the uptake parameter (Figure 3F; one way RM-ANOVA, $F_{(3,3)} = 0.381$, $p = 0.770$). Together, these results suggest that physiological manipulations designed to increase DA release produce the expected effect on the release parameter, with no effect on uptake.

Through their critical roles in the neurotransmitter release process, the effects of altered calcium[20−22] and magnesium[23] ion concentrations are well-understood. Therefore, we determined the effects of altering Ca^{2+}/Mg^{2+} ratios in our model's release parameters. As shown in Figure 4, lowering the Ca^{2+}/Mg^{2+} ratio significantly reduced the r/k_e value (Figure 4A,B; $n = 5$; one-way RM-ANOVA, $F_{(3,12)} = 83.24$, $p < 0.0001$), but it had no significant effect on the uptake parameter, k_u (Figure 4C; one-way RM-ANOVA, $F_{(3,12)} = 1.903$, $p = 0.1830$). As a final pharmacological approach to validate the release parameter, we evaluated the effects of the voltage-dependent sodium channel blocker tetrodotoxin (TTX). As shown in Figure 4D, low concentrations of TTX (10 and 30 nM) reduced the evoked DA responses. Data extracted from the fitted curves indicated that this reduction was due to a significant decrease in the release parameter, r/k_e (Figure 4E; RM-ANOVA, $F_{(2,8)} = 176$; 10 nM TTX, $p < 0.01$ vs control; 30 nM TTX, $p < 0.001$ vs control, Dunnett's posthoc test). In contrast, the uptake parameter, k_u, was not significantly affected by TTX at either concentration (Figure 4F; RM-ANOVA, $F_{(2,8)} = 0.694$, $p = 0.5276$). Together, these experiments indicate that r/k_e is a sensitive measure of DA release. Each of these manipulations also reduced the peak amplitude of the DA signals. However, since the amplitude of the signal is also influenced by uptake, we suggest that r/k_e represents a less ambiguous measure of DA release, especially when drugs with unknown or complex mechanisms of action are to be tested.

Modulation of the Uptake and Release Parameters by Dopamine Transporter Inhibitors. To verify that our model can also quantitatively account for modulation of uptake, we next evaluated the effects of three known DAT inhibitors: cocaine, nomifensine, and the "bath salts" constituent, MDPV. Using FSCV, we previously observed that MDPV is more potent and efficacious than cocaine[24] using an area under the curve analysis that did not distinguish between uptake and release. Consistent with this earlier work, we observed that the effects of MDPV on the DA signal were much more robust than those of cocaine (Figure 5A,B). The extracted uptake parameter, k_u, was plotted as a function of inhibitor concentration. As shown in Figure 5C, MDPV ($n = 7$ slices) was more potent than either cocaine ($n = 8$ slices) or the DAT/norepinephrine transporter (NET) inhibitor nomifensine ($n = 7$ slices). Surprisingly, we also observed that all of these uptake inhibitors significantly enhanced the release parameter r/k_e in a concentration-dependent manner (Figure 5D; MDPV, one-way RM-ANOVA, $F_{(3,18)} = 13.20$; cocaine, one-

DOI: 10.1021/acschemneuro.5b00277
ACS Chem. Neurosci. 2016, 7, 700−709

way RM-ANOVA, $F_{(3,21)}$ = 19.83; nomifensine, $F_{(3,18)}$ = 4.667). As with the inhibition of uptake, MDPV appeared to be more potent than either cocaine or nomifensine at facilitating release. Although cocaine has been suggested to enhance vesicular DA release *in vivo*[25] as well as *in vitro*,[26] our results provide the first evidence that MDPV and nomifensine also increase vesicular DA release. Whether this is due to synapsin-dependent mechanisms, as has been proposed for cocaine,[26] will require additional study. However, our data support the hypothesis that a combination of uptake inhibition and enhanced vesicular release underlies the effects of these DAT inhibitors in vitro.

Effects of Amphetamine on DA Release and Uptake. A recent *in vivo* FSCV study proposed that amphetamine enhances exocytotic DA release,[8] in apparent contrast with the demonstrated ability of this drug to deplete DA vesicles *in vitro*.[27] This paradoxical finding was recently investigated by Siciliano et al.,[9] who concluded that low concentrations (10−200 nM) of amphetamine reduce uptake in brain slices without affecting release. However, the study by Siciliano et al. utilized an analysis of peak amplitude changes in wild-type and DAT knockout mice rather than independent measures of release and uptake.[9] Given these findings, as well as the mixed effects of the uptake inhibitors noted above, we evaluated the actions of amphetamine (300 nM) on release and uptake parameters in our model. As shown in Figure 6, amphetamine significantly reduced the uptake parameter k_u (Figure 6B; n = 9, p = 0.02, paired two-tailed t-test), but it did not significantly affect the release parameter r/k_e (Figure 6A; p = 0.07, paired two-tailed t-test). Thus, our model confirms the findings of Siciliano et al.[9] and is consistent with the known ability of amphetamine to inhibit DAT at low concentrations (K_i = 34 nM[28]). It is important to note, however, that our measurement of r/k_e reflects conventional vesicular release, as evidenced by its sensitivity to TTX and Ca^{2+}/Mg^{2+}. At higher concentrations than those used in the present study, amphetamine is also known to elicit outward, transporter-mediated efflux of DA[29,30] detected using background-subtracted FSCV[31] and other voltammetric approaches.[32] Thus, whereas amphetamine's actions as a DAT inhibitor are readily apparent using our model, we found no evidence for this drug's ability to enhance vesicular DA release.

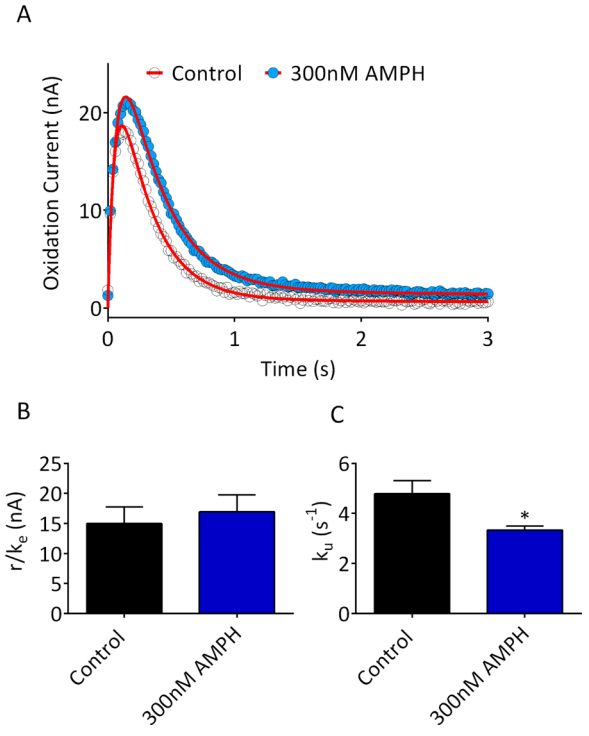

Figure 6. Effect of amphetamine on modeled parameters. (A) Representative recording from a striatal brain slice, prior to (control) and following bath application of 300 nM amphetamine (AMPH). Data represent the mean of three signals obtained under each condition and are plotted with circles. The fitted curves are shown with the red line. (B) Release parameter r/k_e for all slices tested with AMPH (n = 9). No significant difference in release was observed (p = 0.07 vs control, paired two-tailed t-test). (C) Uptake parameter k_u was significantly reduced by 300 nM AMPH (*p = 0.017 vs control, paired two-tailed t-test). Parameter values for the fitted curves are provided in the Supporting Information.

Modulation of DA Release by Kappa Opioid Receptors. The data presented above suggest that r/k_e and k_u are useful in distinguishing between pharmacological manipulations that affect release and uptake, respectively. Although uptake inhibitors, manipulations in external calcium levels, and TTX represent mechanistically distinct ways to affect these processes, the mechanism(s) through which other drugs affect DA release or uptake is still controversial. The presence of KORs on DA axonal profiles,[33,34] coupled with the aversive behavioral effects of KOR activation,[35] has led to the hypothesis that KORs can directly modulate DA release. However, studies utilizing microdialysis[36] or biochemical approaches[37] have suggested that KORs directly interact with DATs and enhance DA uptake. In contrast, earlier *in vitro* FSCV studies strongly suggest that kappa agonists inhibit DA release without affecting uptake.[14,15] Therefore, we evaluated the effects of selective KOR agonist U50,488[15,38] on DA signal parameters. As shown in Figure 7, U50,488 inhibited DA release, as indicated by a significant reduction in the r/k_e parameter (Figure 7B; RM-ANOVA, $F_{(2,10)}$ = 9.42, p = 0.005). In contrast, U50,488 did not significantly affect the uptake parameter k_u (RM-ANOVA, $F_{(2,\ 10)}$ = 0.5017, p = 0.62). Although we cannot discount the possibility that systemic or long-term treatment with KOR agonists might alter DA uptake via altered DAT trafficking,[37] we suggest that the acute inhibitory effects of KOR activation *in vitro* reflect a direct effect on DA release, as previously suggested.[14,15]

Advantages of the Present Model. A major advantage of our model is that it can be applied to nontransformed data using conventional, commercially available software (GraphPad Prism, Origin, SigmaPlot, etc.). In contrast, modeling using Michaelis−Menten kinetics requires first transforming current measurements into concentration. Both time-dependent changes in electrode sensitivity and the postrecording calibration environment[18,19] may influence these measures, thereby adding uncertainty in the conversion of current to DA concentration. Additionally, Michaelis−Menten models make assumptions about the mechanism of inhibitor effects, which is not justified for poorly characterized or novel drugs.[5] Our model is based on the kinetic model proposed by Walters et al.,[11,12] which proposes that DA release first occurs into an inner compartment, followed by transfer into an outer compartment, where the recording electrode measures the oxidation current (see Supporting Information). This model fully accounts for the lag and/or overshoot in the electrode response typically observed during *in vivo* recordings.[12] In the present study, DA is initially detected within 20 ms following local, single-pulse electrical stimulation in the brain slice, and it reaches a maximum within 150−200 ms. Thus, whereas lag is minimal given the proximity of the stimulating and recording electrodes in the slice, there is still a

DOI: 10.1021/acschemneuro.5b00277
ACS Chem. Neurosci. 2016, 7, 700−709

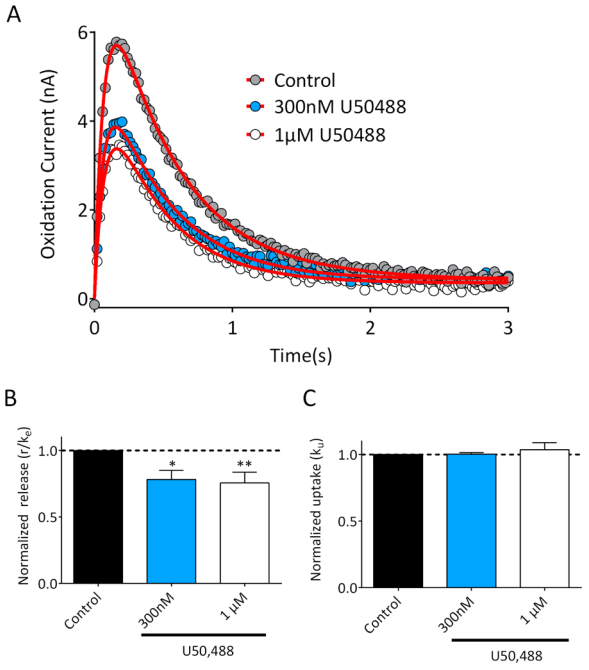

Figure 7. Inhibition of striatal DA release by the kappa opioid receptor. (A) Representative recording from a striatal brain slice demonstrating the effects of 300 nM and 1 μM U50,488. Data represent the mean of three signals obtained under each condition and are plotted with circles. The fitted curves are shown with the red line. (B) Summary of the release parameter, r/k_e ($n = 6$ slices from two rats). U50,488 significantly reduced release at both 300 nM and 1 μM (RM-ANOVA, $F_{(2,10)} = 9.42$, $p = 0.005$; $^{**}p < 0.05$, $^{***}p < 0.01$ vs control, Dunnett's post hoc) . (C) Normalized uptake parameter k_u was not significantly affected by U50,488 (RM-ANOVA, $F_{(2,10)} = 0.5017$, $p = 0.620$). Parameter values for the fitted curves are provided in the Supporting Information.

delay for DA to be fully "transferred" from the release site(s) to the recording electrode. This delay is fully accounted for by the first-order rate constant k_e in our mathematical model, equivalent to the k_T term derived by Walters et al.[11,12] Whereas r and k_e individually reflect complex underlying processes that are difficult to resolve, we demonstrate that the *ratio of these two values* will always yield the DA initially present in the inner compartment (DA_{ic}). Since DA_{ic} itself is directly derived from DA released from the axon terminals,[11,12] solving for DA_{ic} is fundamentally a measure of DA release. We note that r/k_e values are slightly but significantly higher than the peak amplitude of the response, consistent with their relationship to DA release. Importantly, we found that whereas r/k_e and peak amplitude were strongly correlated, only peak amplitude maintained a small but significant correlation with the uptake parameter. In essence, r/k_e provides a correction for the peak amplitude that would otherwise be confounded by ongoing uptake. For this reason, we believe that solving for r/k_e and k_u, as described here, will be beneficial for examining the mechanisms through which various agents alter DA release and uptake as measured by FSCV.

Implications for Drug Abuse. Our results confirm the ability of the psychostimulant cocaine to promote DA release, a process that has been linked to cocaine's interaction with Ca^{2+}-dependent vesicular proteins.[26] We also demonstrate that, in addition to their actions as uptake inhibitors, both MDPV and nomifensine are also able to increase vesicular DA release. The release-promoting effects of MDPV have not been described previously, and it remains to be determined whether the mechanisms underlying this effect are similar to those described previously for cocaine.[25,26] The robust enhancement of vesicular DA release by MDPV, coupled with its ability to potently inhibit uptake, likely contributes to the rewarding properties of this widely abused synthetic cathinone.[39,40] The effects of cocaine, nomifensine, and MDPV on release are also distinct from the actions of amphetamine, which did not promote vesicular release according to our model. Although amphetamine can disrupt vesicular storage[9,41] at higher concentrations (>1 μM) than those used in the present study, we observed no effects on release at the lower concentration tested. Together, these studies help to further discriminate the specific actions of various stimulants on DA release and uptake.

In summary, by applying a simplified model of DA release and uptake with brain slice recordings, we describe a method for distinguishing DA release from uptake using FSCV. The model can be easily implemented using common nonlinear curve-fitting software packages, and it does not require transformation of the data. Our model was validated in brain slices using a variety of physiological and pharmacological manipulations that alter DA release and/or uptake, and we suggest that it may be similarly useful in investigating the actions of any drug or manipulation thought to affect DA signaling dynamics.

METHODS

Subjects. All studies were performed in brain slices obtained from 4 to 5 week old male Sprague−Dawley rats. Studies were approved by the NIDA IRP Animal Care and Use Committee, in accordance with NIH Guidelines.

Brain Slice Preparation. Rats were anesthetized with isoflurane and decapitated, and brains were rapidly removed and placed in ice-cold, oxygenated artificial cerebrospinal fluid (aCSF) consisting of, in mM, NaCl, 126; KCl, 3; $MgCl_2$, 1.5; $CaCl_2$, 2.4; NaH_2PO_4, 1.2; $NaHCO_3$, 26; and glucose, 11. Coronal hemisections (280 μm) containing the striatum were cut using a vibratome (Leica VT1200S, Buffalo Grove, IL, USA). Slices were incubated in standard oxygenated aCSF at 34−35 °C for ∼20 min and allowed to stabilize at room temperature for at least 30 min prior to initiating recordings. During recordings, slices were placed in a small volume recording chamber (RC-26, Warner Instruments), continuously superfused with aCSF at a rate of 2 mL/min using a peristaltic pump, and maintained at 28−30 °C using an in-line solution heater. A manifold containing stopcock valves was used to switch between control and drug-containing aCSF.

Fast-Scan Cyclic Voltammetry. FSCV using carbon fiber electrodes was performed as described previously.[13,42] Carbon fibers (7 μm diameter) were vacuum-aspirated into borosilicate glass pipettes and cut so that ∼25−30 μm exposed surface protruded from the pipet tip. Pipettes were backfilled with a 4 M potassium acetate/150 mM KCl solution and connected to the headstage of a holder/headstage assembly (HEKA EVA-8, Heka Instruments, Holliston, MA). Voltage scans, stimulation protocols, and data acquisition were performed using PCI-based A/D boards and LabView-based software (TarHeel CV, University of North Carolina). Scans consisted of sweeps from −0.4 to 1.3 V and back to −0.4 V, at a rate of 400 V/s, and were obtained at either 10 or 50 Hz. A 5 s control period preceded each electrically evoked response and was used to obtain a background current that was digitally subtracted from the current obtained during the peak of the response. All cyclic voltammograms matched the expected profile of DA. Under stereoscopic magnification, carbon fibers were lowered to a depth of ∼100 μm in the dorsal striatum. A bipolar stimulating electrode, connected to a constant current stimulus isolator (DS-3, Digitimer, Hertfordshire, UK), was positioned ∼75−100 μm from the carbon fiber. Responses were elicited by a single pulse (1 ms, 150−200 μA) every 90 s. Predrug baselines were obtained by averaging three responses prior to drug application. Postdrug responses were taken by averaging the last three responses following a 12 min drug application.

DOI: 10.1021/acschemneuro.5b00277
ACS Chem. Neurosci. 2016, 7, 700−709

Modeling of Measured DA Signals. Prior work has demonstrated that the DA measured at carbon fiber electrodes *in vivo* and *in vitro* reflects the net balance of release, uptake, and diffusional processes.[3−5] Therefore, we began by assuming, as in Walters et al.[11] (their eq 2), that the dopamine concentration at the carbon fiber electrode is described by a first-order differential equation (neglecting "hang-up")

$$d[DA]/dt = r \exp(-k_e \times t) - k_u \times [DA] \quad (1)$$

where r is a release rate parameter, k_e is a rate constant for transfer of DA to the carbon fiber electrode, and k_u is an uptake parameter that comprises both diffusion and transporter-mediated uptake. The solution to this equation (initial $[DA] = 0$) is

$$[DA] = \frac{r(\exp(-k_u \times t) - \exp(-k_e \times t))}{k_e - k_u}$$

If uptake were blocked ($k_u = 0$), then $[DA] = r/k_e$ at $t \to \infty$. In other words, the ratio of parameters r and k_e is simply the DA concentration that would appear at the electrode if all uptake (diffusion and transport) was blocked and time was infinite; r/k_e is the measure of DA released used in this article. Since r is a rate parameter, it is given in units of nA/s or μM/s, and k_e will be given in s^{-1}. Thus, r/k_e will be in units of either nA or μM if it is converted to a concentration by posthoc calibration. The parameter k_u is also expressed in s^{-1}.

In addition to its release, uptake, and diffusion, DA also undergoes adsorption to the electrode surface,[10,11] where it undergoes multiple redox cycles and thereby continues to contribute to the signal. This process, modeled as a first-order adsorption−desorption process, gives rise to the tail or "hang-up"[12] component of the signal

$$d[DA_{ads}]/dt = k_{ads} \times [DA] - k_{des} \times [DA_{ads}] \quad (2)$$

where k_{ads} and k_{des} are adsorption and desorption rate constants, respectively, that have been scaled to fit the data. These two coupled differential equations can be solved for both free and adsorbed dopamine, which are summed as the measured signal

$$[DA]_{meas} = [DA] + [DA_{ads}]$$

This signal function is used to simulate data (Figure 1D−F) or fit to real data by a least-squares algorithm to derive the parameter values. Programs such as MLAB (Civilized Software, Bethesda, MD) can use the system of differential equations above to simulate or fit data. To allow the signals to be simulated or fit by other programs (such as GraphPad Prism or Excel) that cannot readily utilize complex systems of differential equations, the integrated form of these equations may be used (Supporting Information).

Drugs and Reagents. Cocaine hydrochloride, D-amphetamine sulfate, and MDPV were obtained through NIDA Drug Supply. TTX was obtained from Alamone Laboratories (Jerusalem, Israel). U50,488 hydrochloride and nor-BNI were obtained from Tocris. All other reagents and chemicals were obtained from Sigma-Aldrich. Drugs were prepared as stock solutions in water and dissolved freshly before use in aCSF.

Data Analysis. Mean responses were plotted in either MLAB (Civilized Software, Bethesda, MD) or GraphPad Prism (v 6.0, GraphPad Scientific, San Diego, CA). Nonlinear curve fitting, using a least-squares algorithm, was used to calculate parameters for each curve. In nearly all cases, all of the parameters were unconstrained. In a few cases, to improve fitting, k_{ads} or k_{des} was allowed to be a shared parameter within a data set since these parameters reflect a property of the recording electrode (e.g., adsorption) and would not be expected to be affected by pharmacological manipulations. Parameters were normalized to the control (predrug) condition within each slice. Statistical tests were performed using GraphPad Prism, with a critical level of $p < 0.05$ used to determine statistical significance. Posthoc comparisons were performed only when an ANOVA yielded a significant main effect. Tau and 80% decay times of signals were measured using the WinWCP software package (WinWCP v 5.0.8; University of Strathclyde, Glasgow, U.K.; http://spider.science.strath.ac.uk/sipbs/software_ses.htm).

■ ASSOCIATED CONTENT

Supporting Information

The Supporting Information is available free of charge on the ACS Publications website at DOI: 10.1021/acschemneuro.5b00277.

Schematic illustration of the restricted diffusion model described in the present study, the integrated forms of the differential equations for release/uptake and adsorption, an example script of programming syntax for GraphPad Prism, and parameter value tables for all data sets shown in Figures 3−7 (PDF)

■ AUTHOR INFORMATION

Corresponding Author

*Phone: (443) 740-2809. E-mail: ahoffman@mail.nih.gov.

Author Contributions

A.F.H. and C.E.S. designed and performed all experiments, with input from C.R.L. C.E.S. and A.F.H. analyzed data. A.F.H., C.E.S., and C.R.L. wrote the manuscript.

Funding

Support was provided by the NIDA Intramural Research Program.

Notes

The authors declare no competing financial interest.

■ ACKNOWLEDGMENTS

The authors wish to thank Drs. Joseph Cheer and Michael Baumann for their helpful discussions and critical reading of the manuscript, as well as the anonymous reviewers who provided many insightful comments during the preparation of this work.

■ REFERENCES

(1) Keithley, R. B., Takmakov, P., Bucher, E. S., Belle, A. M., Owesson-White, C. A., Park, J., and Wightman, R. M. (2011) Higher sensitivity dopamine measurements with faster-scan cyclic voltammetry. *Anal. Chem. 83*, 3563−3571.

(2) Kile, B. M., Walsh, P. L., McElligott, Z. A., Bucher, E. S., Guillot, T. S., Salahpour, A., Caron, M. G., and Wightman, R. M. (2012) Optimizing the Temporal Resolution of Fast-Scan Cyclic Voltammetry. *ACS Chem. Neurosci. 3*, 285−292.

(3) Wightman, R. M., and Zimmerman, J. B. (1990) Control of dopamine extracellular concentration in rat striatum by impulse flow and uptake. *Brain Res. Rev. 15*, 135−144.

(4) Jones, S. R., Garris, P. A., Kilts, C. D., and Wightman, R. M. (1995) Comparison of dopamine uptake in the basolateral amygdaloid nucleus, caudate-putamen, and nucleus accumbens of the rat. *J. Neurochem. 64*, 2581−2589.

(5) Wu, Q., Reith, M. E., Wightman, R. M., Kawagoe, K. T., and Garris, P. A. (2001) Determination of release and uptake parameters from electrically evoked dopamine dynamics measured by real-time voltammetry. *J. Neurosci. Methods 112*, 119−133.

(6) Ferris, M. J., Calipari, E. S., Mateo, Y., Melchior, J. R., Roberts, D. C., and Jones, S. R. (2012) Cocaine self-administration produces pharmacodynamic tolerance: differential effects on the potency of dopamine transporter blockers, releasers, and methylphenidate. *Neuropsychopharmacology 37*, 1708−1716.

(7) Yorgason, J. T., Espana, R. A., and Jones, S. R. (2011) Demon voltammetry and analysis software: analysis of cocaine-induced alterations in dopamine signaling using multiple kinetic measures. *J. Neurosci. Methods 202*, 158−164.

(8) Daberkow, D. P., Brown, H. D., Bunner, K. D., Kraniotis, S. A., Doellman, M. A., Ragozzino, M. E., Garris, P. A., and Roitman, M. F. (2013) Amphetamine paradoxically augments exocytotic dopamine release and phasic dopamine signals. *J. Neurosci. 33*, 452−463.

DOI: 10.1021/acschemneuro.5b00277
ACS Chem. Neurosci. 2016, 7, 700−709

(9) Siciliano, C. A., Calipari, E. S., Ferris, M. J., and Jones, S. R. (2014) Biphasic mechanisms of amphetamine action at the dopamine terminal. *J. Neurosci. 34*, 5575−5582.
(10) Bath, B. D., Michael, D. J., Trafton, B. J., Joseph, J. D., Runnels, P. L., and Wightman, R. M. (2000) Subsecond adsorption and desorption of dopamine at carbon-fiber microelectrodes. *Anal. Chem. 72*, 5994−6002.
(11) Walters, S. H., Robbins, E. M., and Michael, A. C. (2015) Modeling the Kinetic Diversity of Dopamine in the Dorsal Striatum. *ACS Chem. Neurosci. 6*, 1468−1475.
(12) Walters, S. H., Taylor, I. M., Shu, Z., and Michael, A. C. (2014) A novel restricted diffusion model of evoked dopamine. *ACS Chem. Neurosci. 5*, 776−783.
(13) Good, C. H., Hoffman, A. F., Hoffer, B. J., Chefer, V. I., Shippenberg, T. S., Backman, C. M., Larsson, N. G., Olson, L., Gellhaar, S., Galter, D., and Lupica, C. R. (2011) Impaired nigrostriatal function precedes behavioral deficits in a genetic mitochondrial model of Parkinson's disease. *FASEB J. 25*, 1333−1344.
(14) Britt, J. P., and McGehee, D. S. (2008) Presynaptic opioid and nicotinic receptor modulation of dopamine overflow in the nucleus accumbens. *J. Neurosci. 28*, 1672−1681.
(15) Ehrich, J. M., Messinger, D. I., Knakal, C. R., Kuhar, J. R., Schattauer, S. S., Bruchas, M. R., Zweifel, L. S., Kieffer, B. L., Phillips, P. E., and Chavkin, C. (2015) Kappa Opioid Receptor-Induced Aversion Requires p38 MAPK Activation in VTA Dopamine Neurons. *J. Neurosci. 35*, 12917−12931.
(16) Sykova, E., and Nicholson, C. (2008) Diffusion in brain extracellular space. *Physiol. Rev. 88*, 1277−1340.
(17) Hrabetova, S., and Nicholson, C. (2004) Contribution of dead-space microdomains to tortuosity of brain extracellular space. *Neurochem. Int. 45*, 467−477.
(18) Kume-Kick, J., and Rice, M. E. (1998) Dependence of dopamine calibration factors on media Ca2+ and Mg2+ at carbon-fiber microelectrodes used with fast-scan cyclic voltammetry. *J. Neurosci. Methods 84*, 55−62.
(19) Gerhardt, G., and Hoffman, A. (2001) Effects of recording media composition on the responses of Nafion-coated carbon fiber microelectrodes measured using high-speed chronoamperometry. *J. Neurosci. Methods 109*, 13−21.
(20) Dodge, F. A., Jr., and Rahamimoff, R. (1967) Co-operative action a calcium ions in transmitter release at the neuromuscular junction. *J. Physiol. 193*, 419−432.
(21) Schneggenburger, R., and Neher, E. (2000) Intracellular calcium dependence of transmitter release rates at a fast central synapse. *Nature 406*, 889−893.
(22) Thanawala, M. S., and Regehr, W. G. (2013) Presynaptic calcium influx controls neurotransmitter release in part by regulating the effective size of the readily releasable pool. *J. Neurosci. 33*, 4625−4633.
(23) Del Castillo, J., and Engbaek, L. (1954) The nature of the neuromuscular block produced by magnesium. *J. Physiol. 124*, 370−384.
(24) Baumann, M. H., Partilla, J. S., Lehner, K. R., Thorndike, E. B., Hoffman, A. F., Holy, M., Rothman, R. B., Goldberg, S. R., Lupica, C. R., Sitte, H. H., Brandt, S. D., Tella, S. R., Cozzi, N. V., and Schindler, C. W. (2013) Powerful cocaine-like actions of 3,4-methylenedioxypyrovalerone (MDPV), a principal constituent of psychoactive 'bath salts' products. *Neuropsychopharmacology 38*, 552−562.
(25) Venton, B. J., Seipel, A. T., Phillips, P. E., Wetsel, W. C., Gitler, D., Greengard, P., Augustine, G. J., and Wightman, R. M. (2006) Cocaine increases dopamine release by mobilization of a synapsin-dependent reserve pool. *J. Neurosci. 26*, 3206−3209.
(26) Kile, B. M., Guillot, T. S., Venton, B. J., Wetsel, W. C., Augustine, G. J., and Wightman, R. M. (2010) Synapsins differentially control dopamine and serotonin release. *J. Neurosci. 30*, 9762−9770.
(27) Jones, S. R., Joseph, J. D., Barak, L. S., Caron, M. G., and Wightman, R. M. (1999) Dopamine neuronal transport kinetics and effects of amphetamine. *J. Neurochem. 73*, 2406−2414.
(28) Rothman, R. B., Baumann, M. H., Dersch, C. M., Romero, D. V., Rice, K. C., Carroll, F. I., and Partilla, J. S. (2001) Amphetamine-type central nervous system stimulants release norepinephrine more potently than they release dopamine and serotonin. *Synapse 39*, 32−41.
(29) Sitte, H. H., and Freissmuth, M. (2015) Amphetamines, new psychoactive drugs and the monoamine transporter cycle. *Trends Pharmacol. Sci. 36*, 41−50.
(30) Rothman, R. B., and Baumann, M. H. (2003) Monoamine transporters and psychostimulant drugs. *Eur. J. Pharmacol. 479*, 23−40.
(31) Jones, S. R., Gainetdinov, R. R., Wightman, R. M., and Caron, M. G. (1998) Mechanisms of amphetamine action revealed in mice lacking the dopamine transporter. *J. Neurosci. 18*, 1979−1986.
(32) Burrell, M. H., Atcherley, C. W., Heien, M. L., and Lipski, J. (2015) A Novel Electrochemical Approach for Prolonged Measurement of Absolute Levels of Extracellular Dopamine in Brain Slices. *ACS Chem. Neurosci. 6*, 1802−1812.
(33) Svingos, A. L., Chavkin, C., Colago, E. E., and Pickel, V. M. (2001) Major coexpression of kappa-opioid receptors and the dopamine transporter in nucleus accumbens axonal profiles. *Synapse 42*, 185−192.
(34) Svingos, A. L., Colago, E. E., and Pickel, V. M. (1999) Cellular sites for dynorphin activation of kappa-opioid receptors in the rat nucleus accumbens shell. *J. Neurosci. 19*, 1804−1813.
(35) Bals-Kubik, R., Ableitner, A., Herz, A., and Shippenberg, T. S. (1993) Neuroanatomical sites mediating the motivational effects of opioids as mapped by the conditioned place preference paradigm in rats. *J. Pharmacol Exp. Ther. 264*, 489−495.
(36) Chefer, V. I., Czyzyk, T., Bolan, E. A., Moron, J., Pintar, J. E., and Shippenberg, T. S. (2005) Endogenous kappa-opioid receptor systems regulate mesoaccumbal dopamine dynamics and vulnerability to cocaine. *J. Neurosci. 25*, 5029−5037.
(37) Kivell, B., Uzelac, Z., Sundaramurthy, S., Rajamanickam, J., Ewald, A., Chefer, V., Jaligam, V., Bolan, E., Simonson, B., Annamalai, B., Mannangatti, P., Prisinzano, T. E., Gomes, I., Devi, L. A., Jayanthi, L. D., Sitte, H. H., Ramamoorthy, S., and Shippenberg, T. S. (2014) Salvinorin A regulates dopamine transporter function via a kappa opioid receptor and ERK1/2-dependent mechanism. *Neuropharmacology 86*, 228−240.
(38) Rothman, R. B., France, C. P., Bykov, V., De Costa, B. R., Jacobson, A. E., Woods, J. H., and Rice, K. C. (1989) Pharmacological activities of optically pure enantiomers of the kappa opioid agonist, U50,488, and its cis diastereomer: evidence for three kappa receptor subtypes. *Eur. J. Pharmacol. 167*, 345−353.
(39) Schindler, C. W., Thorndike, E. B., Goldberg, S. R., Lehner, K. R., Cozzi, N. V., Brandt, S. D., and Baumann, M. H. (2015) Reinforcing and neurochemical effects of the "bath salts" constituents 3,4-methylenedioxypyrovalerone (MDPV) and 3,4-methylenedioxy-N-methylcathinone (methylone) in male rats. *Psychopharmacology (Berl)*, 1−10.
(40) Bonano, J. S., Glennon, R. A., De Felice, L. J., Banks, M. L., and Negus, S. S. (2014) Abuse-related and abuse-limiting effects of methcathinone and the synthetic "bath salts" cathinone analogs methylenedioxypyrovalerone (MDPV), methylone and mephedrone on intracranial self-stimulation in rats. *Psychopharmacology (Berl) 231*, 199−207.
(41) Sulzer, D., Chen, T. K., Lau, Y. Y., Kristensen, H., Rayport, S., and Ewing, A. (1995) Amphetamine redistributes dopamine from synaptic vesicles to the cytosol and promotes reverse transport. *J. Neurosci. 15*, 4102−4108.
(42) Chen, Y. H., Harvey, B. K., Hoffman, A. F., Wang, Y., Chiang, Y. H., and Lupica, C. R. (2007) MPTP-induced deficits in striatal synaptic plasticity are prevented by glial cell line-derived neurotrophic factor expressed via an adeno-associated viral vector. *FASEB J. 22*, 261−275.

DOI: 10.1021/acschemneuro.5b00277
ACS Chem. Neurosci. 2016, 7, 700−709